ELSEVIER

Soil Dynamics and Earthquake Engineering 22 (2002) 371–387

SOIL DYNAMICS AND EARTHQUAKE ENGINEERING

www.elsevier.com/locate/soildyn

Site assessment and evaluation of spatial earthquake ground motion of Kyeongju

Dong-Soo Kim[a,*], Choong-Ki Chung[b,1], Chang-Guk Sun[b], Eun-Seok Bang[a]

[a]Department of Civil Engineering, Korea Advanced Institute of Science and Technology, Kusong-dong, Yusong-gu, Taejŏn 305-701, South Korea
[b]School of Civil, Urban and Geosystem Engineering, Seoul National University, San 56-1, Shinlim-dong, Kwanak-gu, Seoul 151-742, South Korea

Accepted 25 March 2002

Abstract

The earthquake hazard has been evaluated for 10 km × 10 km area around Kyeongju. The ground motion potentials were determined based on equivalent linear analysis by using the data obtained from in situ and laboratory tests. In situ tests include 16 boring investigations, 4 crosshole, 12 downhole, 26 spectral analysis of surface waves tests, and in the laboratory, resonant column tests were performed. The peak ground accelerations range between 0.141g and 0.299g on collapse level earthquake and between 0.050g and 0.120g on operation level earthquake, respectively, showing the high potential of amplification in the deep alluvial layer in Kyeongju area. Distribution maps of site amplification for the peak acceleration, amplification factors (F_a and F_v) and dominant site period of Kyeongju are constructed using geographic information system tools. The amplification factor based on the Korean seismic design guide underestimated the motion in short range and overestimated the motion in mid-period range in Kyeongju. The importance of site-specific analysis and the need for the improved site characterization method are introduced.

Keywords: Seismic hazard; Earthquake ground motion; Ground response analysis; Site amplification; Site characterization; Geographic information system

1. Introduction

When an earthquake occurs, seismic waves radiate away from the source and reach the ground surface on which waves produce shaking. The surface ground shaking, which man has practically experienced, is capable of causing seismic hazard such as casualties and property damage. Although sites are in the same distance from the source of an earthquake, the extent of the seismic hazards results from the seismic load at a particular site which greatly depends upon the characteristics of the site. In particular, soft soil deposits on bedrock tend to amplify significantly the seismic motion at certain frequencies. As one of the most important aspects in geotechnical earthquake engineering practice involves evaluation of the effects of local soil conditions on surface ground motion [5,11], the analysis for seismic sensitivity of ground has been frequently executed and geographic information system (GIS) is now extensively used for the effective and distinctive counter plan against seismic hazards [8].

Since few earthquake motions which have substantial magnitudes and intensities were recorded in Korea, the earthquake ground motions in the seismic design guide were determined based on the relations between the ground motions and earthquake intensities in the historical earthquake events. Most of the historical earthquake events were experienced at the ground surface of the soil sites and the effects of site amplification were possibly included in the earthquake intensities. Therefore, the quantitative evaluation of site amplification considering local site effects is essential, because it can estimate the rock-outcrop motion based on historical earthquakes intensities as well as it can identify the potential consequences of an earthquake.

Kyeongju was the old capital of Shinla Kingdom for 1000 years and has been designated as one of the world's 10 historic sites by UNESCO. In this study, Kyeongju was selected for the evaluation of earthquake ground motion, because Kyeongju is located near the Yangsan Fault which is possibly active and has abundant historical earthquake events. For the site characterization, both in situ and laboratory tests were performed. In situ tests include 16 boring investigations, 4 crosshole, 12 downhole and 26 spectral analysis of surface waves (SASW) tests, and in

* Corresponding author. Tel.: +82-42-869-3619; fax: +82-42-869-3610.
E-mail addresses: dskim@kaist.ac.kr (D.-S. Kim), geolabs@gong.snu.ac.kr (C.-K. Chung), pungsun@gong.snu.ac.kr (C.-G. Sun), silvston@kaist.ac.kr (E.-S. Bang).
[1] Tel.: +82-2-880-7347; fax: +82-2-875-6933.

PII: S0267-7261(02)00023-4

the laboratory, resonant column tests were performed. Ground response analyses were performed at 28 locations based on equivalent linear scheme using El Centro and Artificial earthquake motions and linear analyses were also carried out for comparison. Ground accelerations determined by response analyses were interpreted using GIS tool and the evaluated response spectra and the site amplification factors at short- and mid-periods were compared with those specified in the Korean seismic design guide.

2. Application of GIS

For analysis of the seismic sensitivity in geotechnical earthquake engineering, a third spatial dimension and a fourth temporal dimension are readily desired [1]. The variable spatial data, such as site investigation data including the borehole logs, seismic test data and the pre-existing borehole logs, and the digital cadastral data for exact spatial information, were collected for assessing synthetically the earthquake hazard in Kyeongju. But these data, especially borehole logs and seismic tests data, are point data in two-dimensional plane and line data in three-dimensional space. Therefore, for the spatial earthquake hazard analysis in three-dimensional space, the evaluations such as interpolations and extrapolations of the discrete data collected are required and the database managements, such as storage, update and retrieval of the information stored as data items, are also needed together with effective visualizing scheme. These critical needs are satisfied in current three-dimensional GIS.

In this study, as a framework for the geotechnical earthquake hazard assessment in Kyeongju, GIS tool, which was environmental visualization system (EVS), was utilized in the interpolations and extrapolations of geologic layers, bedrock profile with depth and other geologic and geotechnical information and the building of topographic surface with triangulated irregular networks (TIN) from the digital cadastral data and the superposition of each analyzed layer were also carried out in GIS tool. The method chosen for interpolating the spatial data is kriging, which is known as the optimal interpolation method in the geological and geotechnical predictions in space [13]. Kriging is essentially a geostatistical method of estimation by local weighted averaging. It is less arbitrary than other interpolation methods because the kriging weights are determined by the variogram which is the function to represent the variance of spatial data values and the configuration of the data.

3. Geological and topographical information

Kyeongsang Basin in southeastern part of Korea where Kyeongju is located, is a sedimentary basin that was formed from the latter Jurassic period when Daebo Orogeny occurred to the Cretaceous period of the Mesozoic in land. The basin is composed of sedimentary rock, volcanic rock by extensive volcanic activities and intrusive granite. Particularly, Kyeongju is mainly composed of the intrusion of granite and partially composed of volcanic rock, sedimentary rock such as sandstone and shale, and hornfels by contact metamorphism. Volcanic rock is classified as upper rhyolite and lower andesite and, tuffaceous conglomerate, sandstone and shale are formed between these two volcanic rocks. Granite is classified as granodiorite, biotite granite and hornblende granite and their mineral compositions are quartz, plagioclase, biotite and hornblende, which are extremely transmuted. In general, rock outcrop is significantly weathered. In the boundary between the rocks of Kyeongju and the sedimentary rocks of the Teritary in nearby area, unconformity and fault are frequently observed. This represents the past frequent earthquake activities and the high potential of the future earthquake.

The topography of Kyeongju is characterized as a basin of the plains and low hills in which the downtown and farms are located, with surrounding mountains. Across the area the Hyeongsan River flows northward and several creeks from valleys join the river (Fig. 1). Waterways in the basin are now restricted within a narrow area by flood control for residence. However, according to historical records [9], North creek across the basin was frequently in flood that resulted in the submersion and drift of private houses since the early years of Shinla Kingdom and the major part of Kyeongju basin was flooding area. Therefore the subsurface deposits of Kyeongju can be mainly composed of thick alluvium over bedrock influenced by rivers and creeks.

4. Site investigation and characterization

To evaluate the spatial earthquake ground motions, various site investigations were performed for 10 km × 10 km area which includes the historic sites and current downtown area in Kyeongju. For the geotechnical site characterization, 16 boring investigations, 12 downhole tests, 4 crosshole tests, and 26 SASW tests were executed in total 28 sites of which 4 river beds, 8 hill sides and 16 plain sites were chosen considering the effect of the topography on spatial variations of subsoil properties. The drilling of an exploratory borehole at each site was performed to the depth of 4 m below soft rock (i.e. the engineering rock underlying weathered rock is named soft rock in Korea) for determining the property of bedrock from seismic tests. In addition, the pre-existing 135 boring data mostly gathered from the high-speed rail construction site along the Hyeongsan River were utilized. Locations of borings and contents of seismic tests in the region of study are shown in Fig. 1. To obtain the more detailed information, site investigations in the second phase study were concentrated for 6 km × 6 km area as shown in Fig. 1.

In the laboratory, X-ray diffraction analysis for determining mineral compositions was performed and the degree of

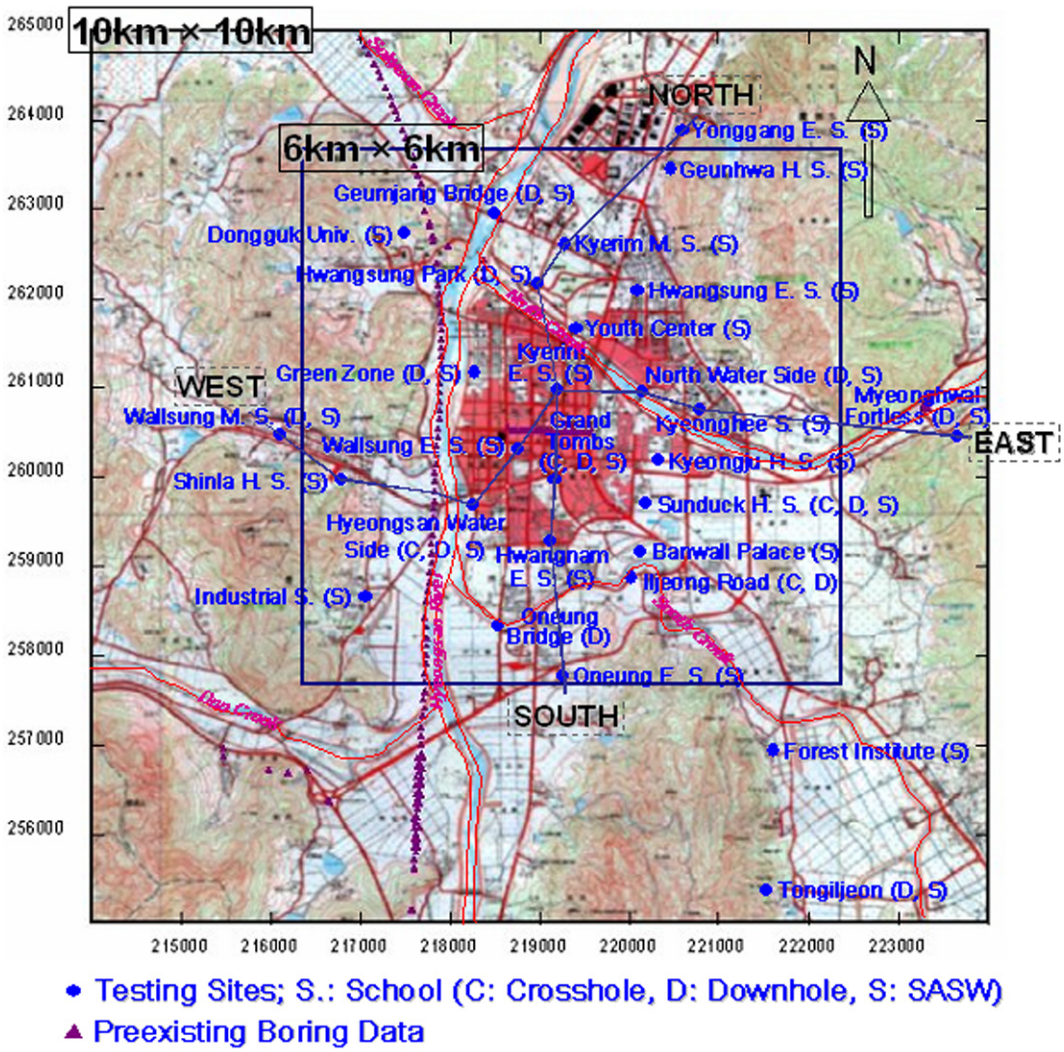

Fig. 1. Location and contents of site investigation in Kyeongju.

weathering was analyzed. Index property tests and direct shear tests for soil strength were executed and resonant column tests for obtaining dynamic soil properties were additionally performed.

The subsurface deposits were investigated by either borings or SASW tests, and typical subsurface layers are plotted in Fig. 2. In the boring investigations, the boundary between the weathered residual soil and weathered rock was classified by 50 blow counts per 15 cm penetration in SPT and the boundary between the weathered rock and soft rock was classified by the degree of drilling capability and the visual observations of the collected samples. In the SASW test sites, subsurface layers were classified by the criteria based on the relationship between each layer and shear wave velocities, which is established from direct comparison between SASW and boring results. The subsurface layers were composed of 10–40 m thickness of alluvial sands and/or gravels over the weathered residual soils in most sites except the mountain areas, because of the historical frequent flooding along the river and creeks. Therefore, the sites are potentially susceptible for the amplification of ground motion during earthquakes.

Figs. 3 and 4 show, respectively, west–east section and north–south section profiles including the depth to the weathered rock and soft rock for geological basin in Kyeongju. Although the exact profiles cannot be predicted owing to small number of site investigation data, the west–east section shows approximately the geological basin which corresponds to the topography. But, the geological basin in north–south section is obscure because of the limited number of boring data, and partially due to the effect of topography (i.e. the plain area is spread in the south).

A result of X-ray diffraction analysis shows that the weathered residual soils and the weathered rock are composed of quartz, orthoclase, and biotite as main minerals and of chlorite, kaolinite and montmorillonite as clay minerals, indicating the parent rock is granite. In addition, index of degree of decomposition, X_d [10], was determined by the examination of minerals with a microscope for estimating the degree of weathering, and the indexes of the

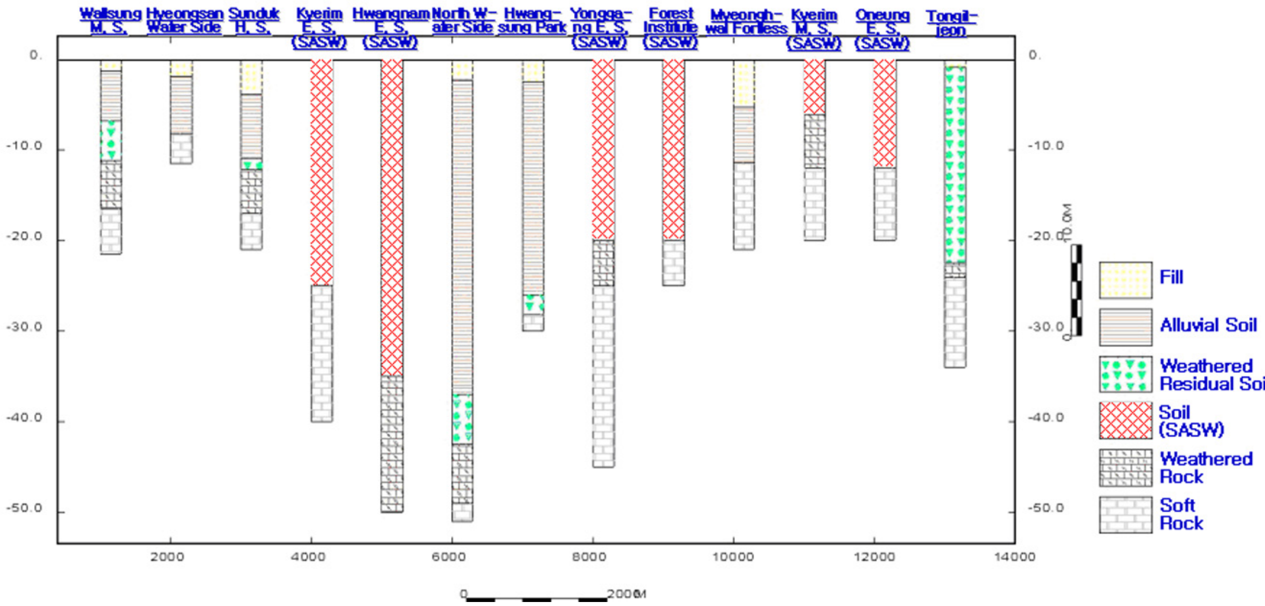

Fig. 2. Typical subsurface layers at each site.

weathered residual soils and the weathered rock are estimated to be about 0.6 and 0.4, respectively.

The alluvial soils are classified as either sand or gravels such as GP, GM, SP, SW, and SM in the unified soil classification system and the friction angles and cohesions range from 30 to 45° and 0.0 to 0.4 kg/cm^2, respectively. The weathered residual soils are classified as SW and SM and the friction angles and cohesions range from 34 to 50° and 0.0 to 0.3 kg/cm^2, respectively.

Figs. 5 and 6 show the variations of normalized shear moduli (G/G_{max}) and damping ratios (D) with shearing strain amplitude for the alluvial and weathered residual soils, respectively. These data were determined by the resonant column tests with reconstituted specimens considering in situ conditions. For ground response analysis, the representative normalized shear modulus reduction and damping curves of each alluvial and weathered residual soils were determined as shown in the figures. The representative

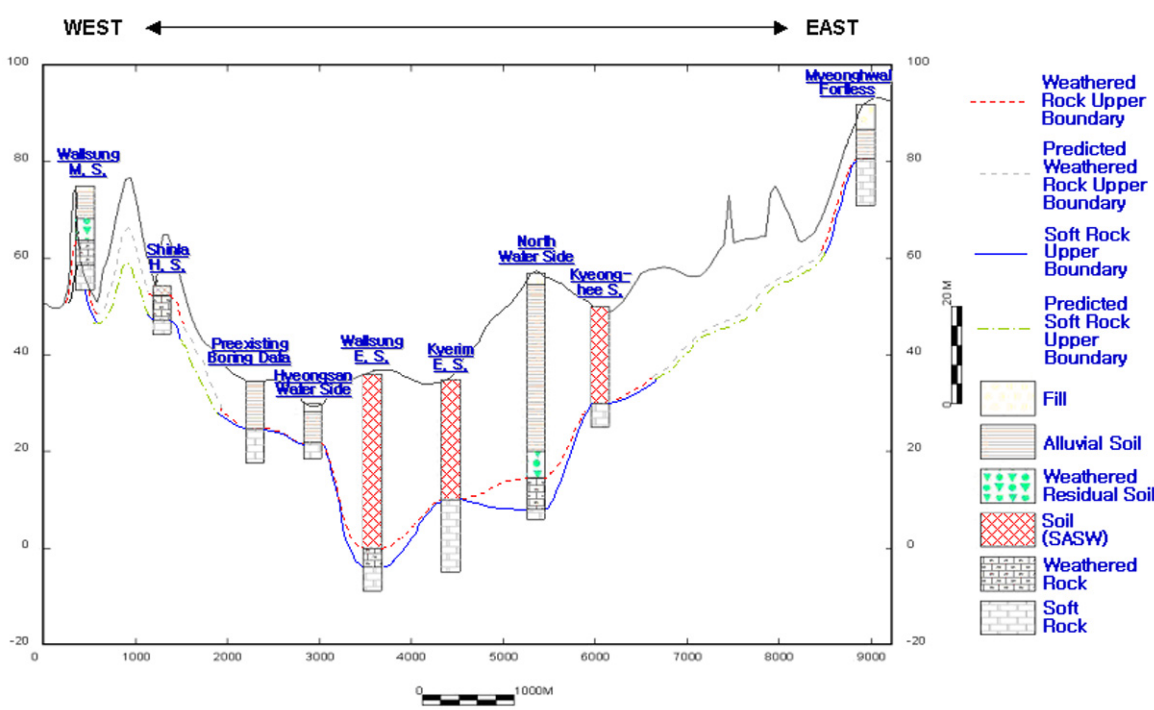

Fig. 3. West–east section profiles of studied area.

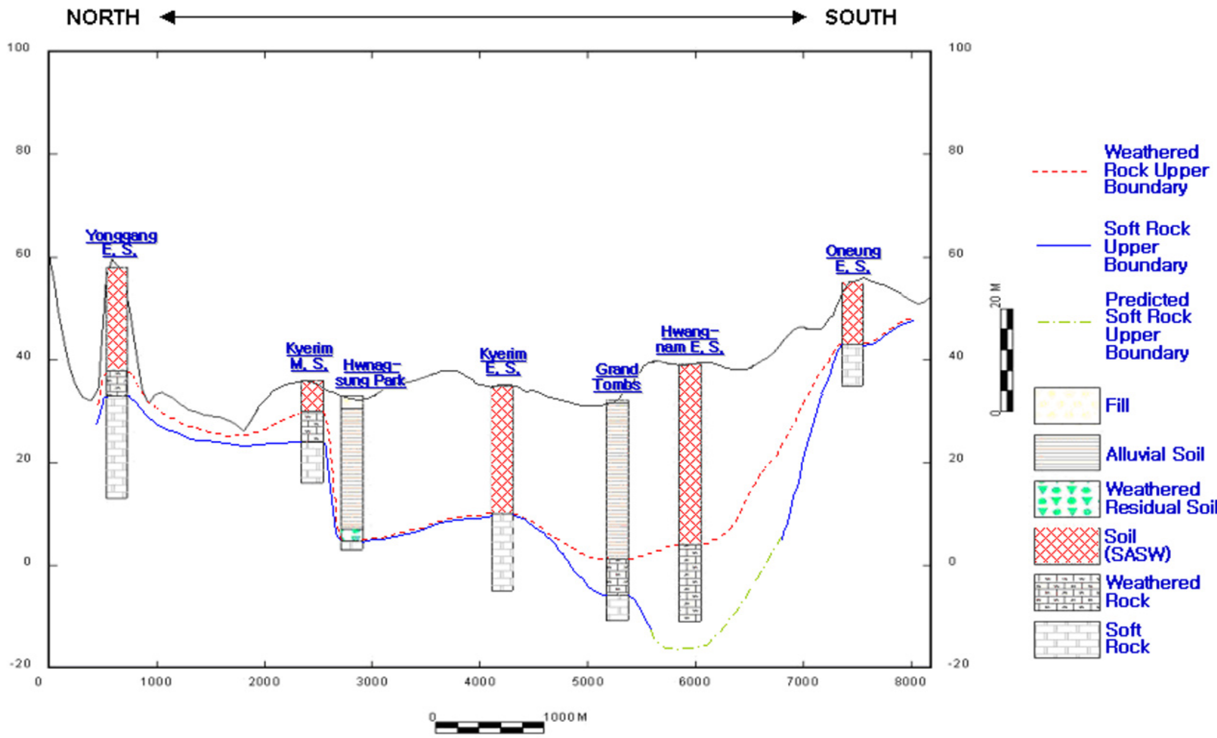

Fig. 4. North–south section profiles of studied area.

G/G_{max} and D curves were fitted to strain level 1% by Ramberg–Osgood Model because of the strain limitation in the resonant column test.

Three kinds of in situ seismic tests (Crosshole, Downhole, SASW tests) were performed to obtain reliable representative shear wave velocity (V_S) profiles. The representative shear wave velocity profiles were determined and used as input data of equivalent linear and linear analyses according to the reliability of testing methods and field testing conditions. Fig. 7 shows the typical representative shear wave velocity profiles based on the combination of in situ seismic tests.

The site conditions can be characterized as six categories according to the mean shear wave velocity ($\bar{V}_S$) of the upper 30 m as suggested in the Korean seismic design guide [12]. Most of the area in Kyeongju was found to be S_B (Rock; $760 < \bar{V}_S \leq 1500$ m/s), S_C (very stiff soil or soft rock; $360 < \bar{V}_S \leq 760$ m/s) or S_D (stiff soil; $180 < \bar{V}_S \leq 360$ m/s) based on $\bar{V}_S$ determined by in situ seismic tests. Fig. 8 shows the distribution map of the mean shear wave velocity of the upper 30 m in the studied area using GIS tools. GIS mapping was performed for 10 km × 10 km area, but only 6 km × 6 km area where authors were mainly concerned,

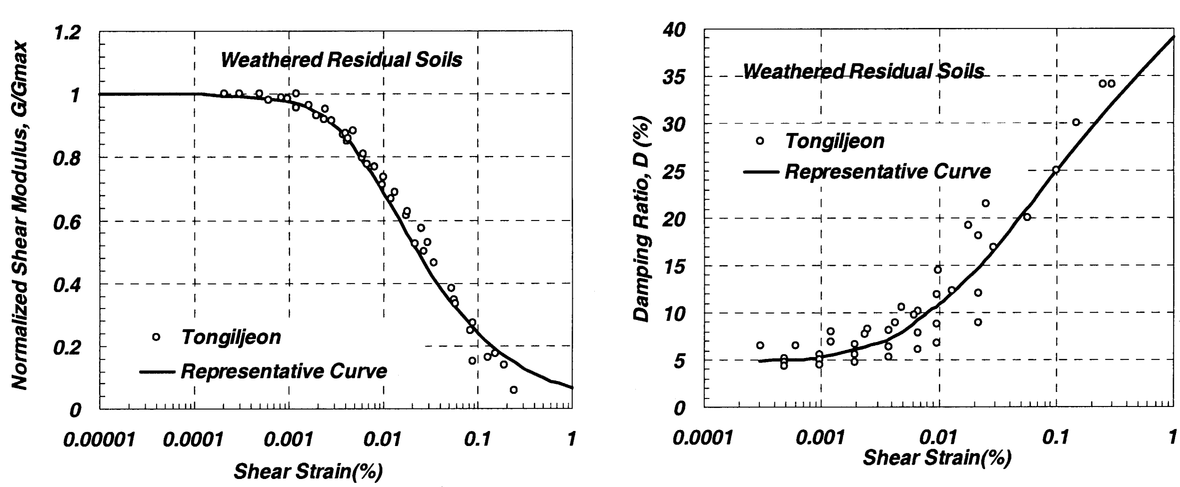

Fig. 5. Representative normalized shear modulus and damping ratio curves of alluvial soils.

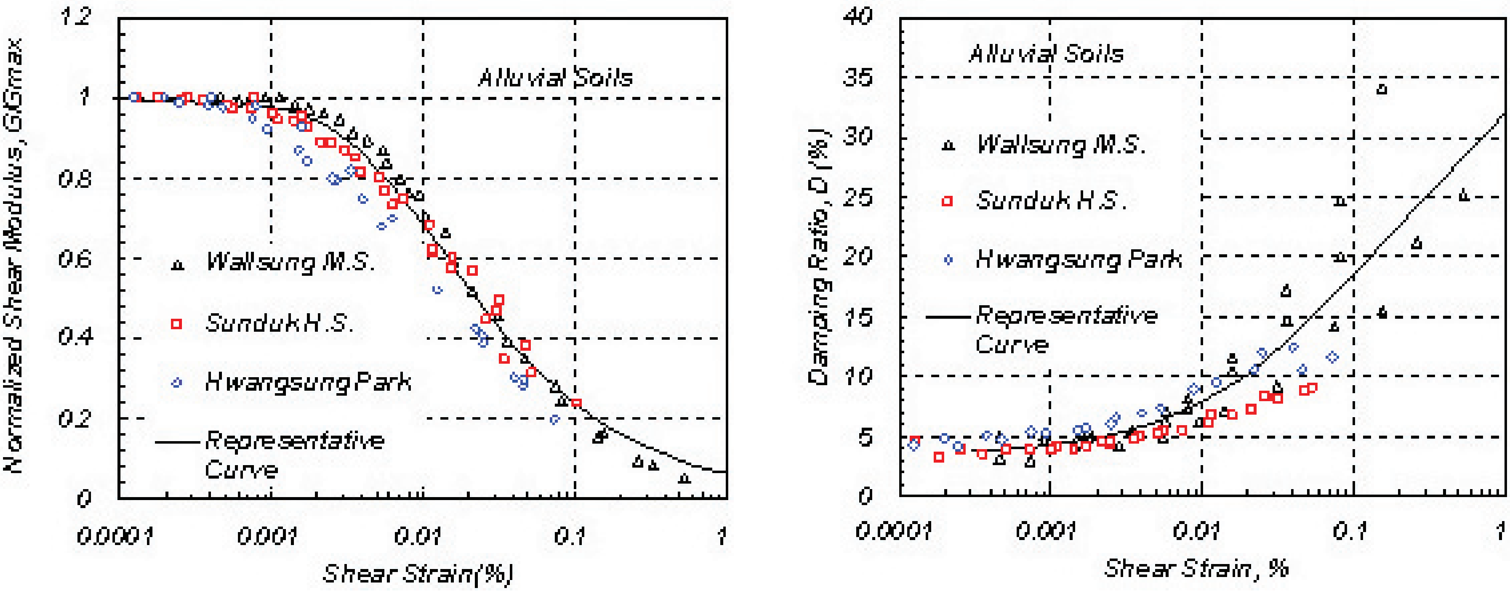

Fig. 6. Representative normalized shear modulus and damping ratio curves of weathered residual soils.

was shown in the figures. The mountain area has the high mean shear wave velocity, which is categorized as S_B while the basin area, mostly downtown of city, has the low mean shear wave velocity, which is categorized as S_C and S_D, showing high potential of site amplification.

5. Results of ground response analysis

Site response analysis was performed based on equivalent linear scheme using SHAKE91 [6] for considering nonlinear properties of soil, and linear analysis was also performed for comparison purposes. The equivalent linear analysis will provide relatively reliable results when strain level caused by earthquake is lesser than 1%, which is a typical range in the moderate seismic zone such as in Kyeongju.

Because the ground motion is significantly affected by the local geologic conditions, the composition of the entire soil column determined by individual borings was separately utilized in the analysis. The design rock-outcrop accelerations for seismic category I structures at Kyeongju are 0.14g at collapse level earthquake (CLE; 1000 year return period) and 0.05g at operation level earthquake (OLE; 100 year return period) based on Korean seismic hazard map. Input soil parameters such as maximum shear modulus, mass density and G/G_{max} reduction and damping curves were

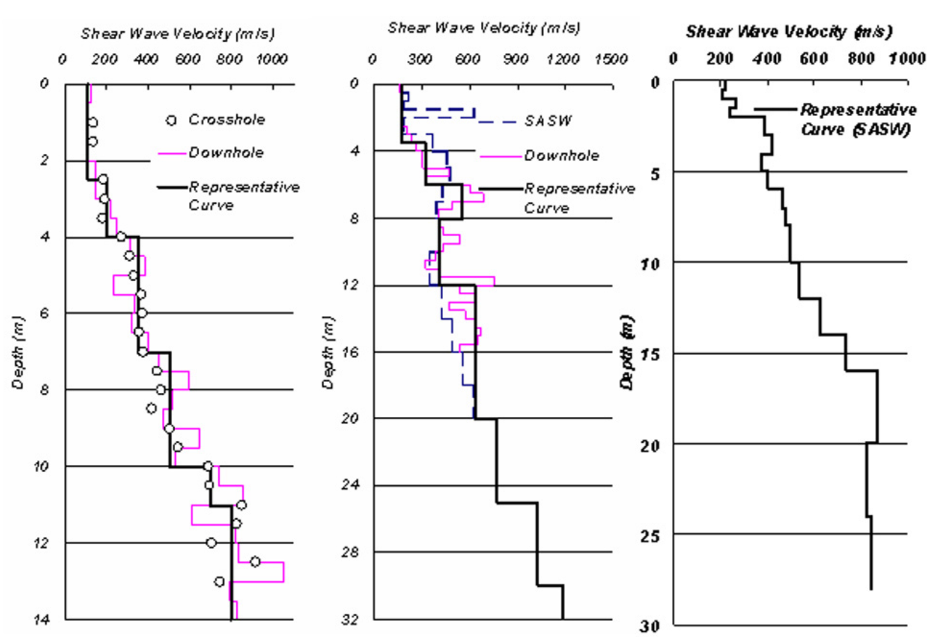

Fig. 7. Typical representative shear wave velocity profiles.

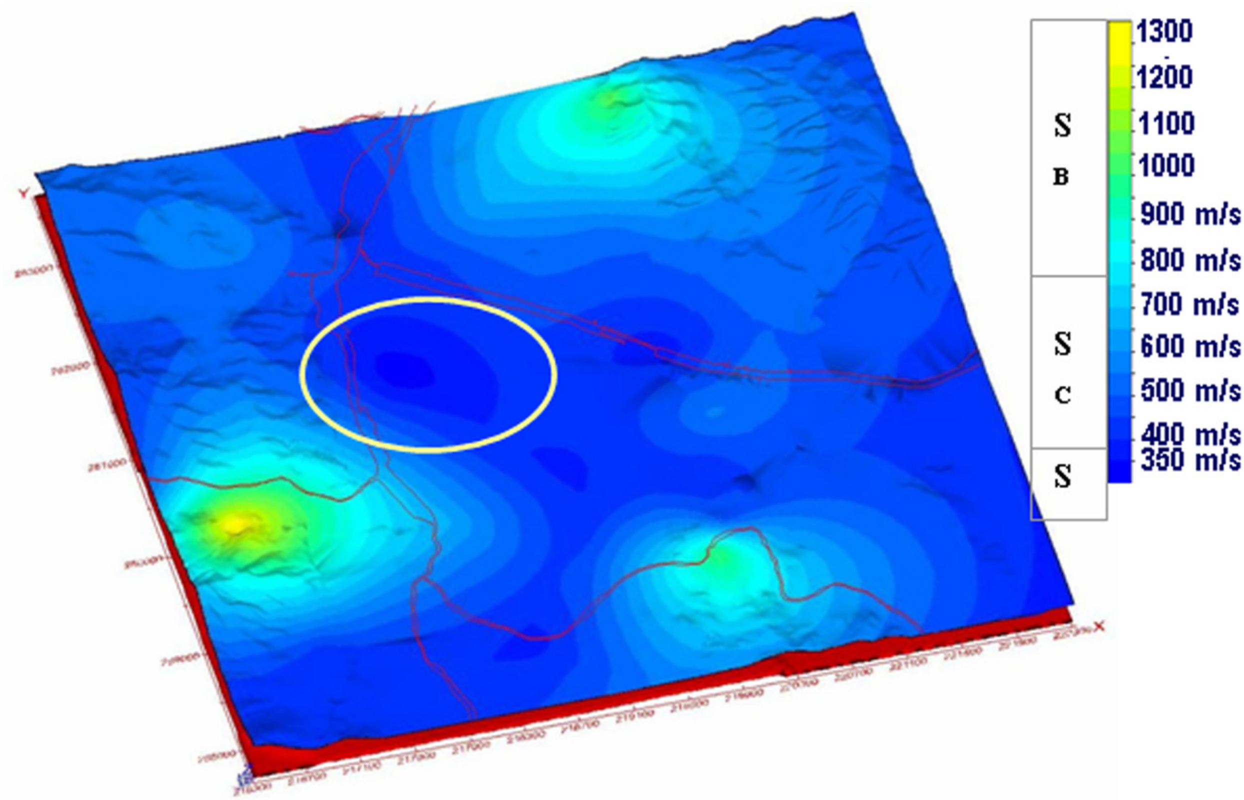

Fig. 8. Distribution map of the mean shear wave velocity of the upper 30 m for the 6 km × 6 km area.

determined at each layer and the bedrock properties ranged from 800 to 1000 m/s of shear wave velocity determined from borehole seismic and SASW tests. The velocities of bedrock fall into the property ($V_S > 750$ m/s) of the seismic engineering rock [2]. Depths to bedrock of each site are summarized in Tables 1 and 2. El Centro and Artificial earthquake motions (Fig. 9) which were modified to the level of the design rock-outcrop acceleration were used as input earthquake. The peak ground accelerations were determined at each soil column and tabulated in Tables 1 and 2.

The peak ground accelerations range between 0.141*g* and 0.299*g* on CLE, and between 0.050*g* and 0.120*g* on OLE, respectively. Depending on site conditions, the maximum of 2.4 times site amplification is expected and the deep alluvial

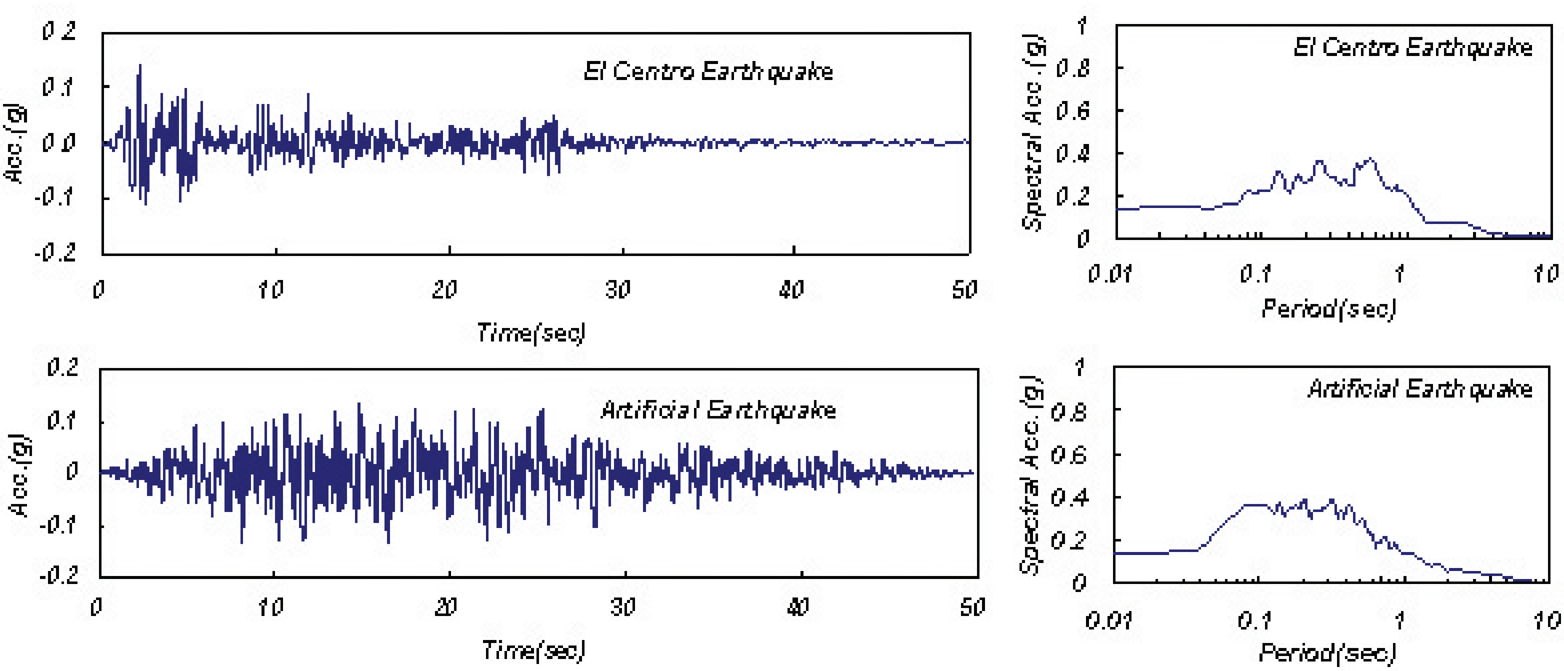

Fig. 9. Acceleration–time histories and response spectra of input earthquakes on CLE.

Table 1
Summary results of site response analyses at Kyeongju (El Centro EQ) (V_S^*: the average value of V_S to bed rock)

Sites	Depth to bed rock, H (m)	Mean V_S of upper 30 m (m/s)	Mean V_S^* (m/s)	Soil type	Resonance frequency			Max. strain level (%)		Ground acc. (g)	
					$f = V_S^*/4H$	SHAKE					
						CLE	OLE	CLE (0.14g)	OLE (0.05g)	CLE (0.14g)	OLE (0.05g)
Hyeongsan River	8	661	253	S_C	7.9	9.8	11.0	0.018	0.005	0.244	0.088
Sunduk H.S.	11	429	248	S_C	5.6	6.3	7.3	0.068	0.018	0.286	0.116
Wallsung M.S.	18	381	267	S_C	3.7	2.8	3.3	0.401	0.049	0.165	0.075
Tongiljeon	31	372	372	S_C	3.0	3.6	4.1	0.042	0.010	0.218	0.090
North Creek	45	366	366	S_C	2.0	2.5	3.0	0.070	0.015	0.229	0.092
Hwangsung Park	28	456	410	S_C	3.7	4.9	5.4	0.056	0.011	0.276	0.102
Myeonghwal Fortless	16	357	245	S_D	3.8	3.0	4.0	0.166	0.029	0.183	0.087
Forest Institute	25	347	297	S_D	3.0	2.5	3.4	0.104	0.016	0.180	0.086
Oneung E.S.	14	560	374	S_C	6.7	7.0	7.9	0.020	0.005	0.224	0.074
Yonggang E.S.	30	359	359	S_D	3.0	2.6	3.5	0.156	0.030	0.223	0.091
Hwangnam E.S.	50	412	412	S_C	2.1	1.9	2.3	0.047	0.010	0.169	0.058
Kyerim E.S.	25	420	385	S_C	3.9	3.3	4.1	0.047	0.009	0.158	0.067
Kyerim M.S.	14	641	408	S_C	7.3	9.6	10.1	0.016	0.005	0.226	0.081
Iljeong Road	5	1019	428	S_B	21.4	23.1	23.8	0.006	0.002	0.142	0.050
Green zone	35	311	339	S_D	2.4	1.3	1.8	0.653	0.206	0.183	0.087
Geumjang Bridge	32	408	405	S_C	3.2	4.1	4.8	0.034	0.009	0.284	0.105
Grand Tombs	38	385	424	S_C	2.8	2.6	3.3	0.095	0.024	0.239	0.095
Dongguk Univ.	16	581	395	S_C	6.2	5.6	6.5	0.037	0.009	0.207	0.083
Oneung Bridge	30	378	378	S_C	3.2	3.4	4.0	0.040	0.011	0.263	0.114
Geunhwa H.S.	1.5	1053	286	S_B	47.7	54.9	54.9	0.002	0.001	0.141	0.050
Hwangsung E.S.	12	521	337	S_C	7.0	5.0	6.6	0.094	0.014	0.173	0.066
Kyeongju H.S.	16	563	436	S_C	6.8	8.0	8.5	0.006	0.002	0.183	0.065
Kyeonghee S.	20	506	420	S_C	5.3	6.4	6.9	0.031	0.010	0.236	0.088
Industrial S.	36	439	468	S_C	3.3	4.0	4.5	0.096	0.018	0.266	0.108
Shinla H.S.	7	1239	617	S_B	22.0	22.4	22.8	0.004	0.001	0.143	0.051
Youth Center	16	487	354	S_C	5.5	6.1	6.9	0.016	0.005	0.241	0.088
Wallsung E.S.	40	411	447	S_C	2.8	2.8	3.3	0.027	0.007	0.226	0.081
Banwall Palace	14	466	264	S_C	4.7	4.5	5.8	0.226	0.040	0.253	0.109

Table 2
Summary results of site response analyses at Kyeongju (Artificial EQ) (V_S^*: the average value of V_S to bed rock)

Sites	Depth to bed rock, H (m)	Mean V_S of upper 30 m (m/s)	Mean V_S^* (m/s)	Soil type	Resonance frequency			Max. strain level (%)		Ground acc. (g) Artificial EQ	
					$f = V_S^*/4H$	SHAKE					
						CLE	OLE	CLE (0.14g)	OLE (0.05g)	CLE (0.14g)	OLE (0.05g)
Hyeongsan River	8	661	253	S_C	7.9	9.4	10.9	0.026	0.006	0.281	0.106
Sunduk H.S.	11	429	248	S_C	5.6	6.0	7.1	0.081	0.019	0.299	0.118
Wallsung M.S.	18	381	267	S_C	3.7	3.0	3.4	0.299	0.058	0.176	0.085
Tongiljeon	31	372	372	S_C	3.0	3.5	4.1	0.052	0.012	0.211	0.086
North Creek	45	366	366	S_C	2.0	2.6	3.0	0.076	0.015	0.215	0.082
Hwangsung Park	28	456	410	S_C	3.7	4.8	5.4	0.067	0.010	0.271	0.094
Myeonghwal Fortless	16	357	245	S_D	3.8	3.0	4.0	0.151	0.030	0.201	0.095
Forest Institute	25	347	297	S_D	3.0	2.8	3.5	0.071	0.016	0.198	0.086
Oneung E.S.	14	560	374	S_C	6.7	7.0	7.9	0.020	0.005	0.225	0.086
Yonggang E.S.	30	359	359	S_D	3.0	2.8	3.5	0.164	0.032	0.200	0.094
Hwangnam E.S.	50	412	412	S_C	2.1	2.0	2.4	0.025	0.007	0.142	0.057
Kyerim E.S.	25	420	385	S_C	3.9	3.5	4.1	0.038	0.009	0.175	0.070
Kyerim M.S.	14	641	408	S_C	7.3	9.5	10.0	0.019	0.006	0.272	0.093
Iljeong Road	5	1019	428	S_B	21.4	23.0	23.8	0.007	0.048	0.167	0.059
Green zone	35	311	339	S_D	2.4	1.5	2.0	0.384	0.002	0.116	0.077
Geumjang Bridge	32	408	405	S_C	3.2	4.3	4.8	0.038	0.009	0.272	0.109
Grand Tombs	38	385	424	S_C	2.8	2.8	3.4	0.133	0.025	0.255	0.104
Dongguk Univ.	16	581	395	S_C	6.2	5.4	6.5	0.054	0.010	0.238	0.082
Oneung Bridge	30	378	378	S_C	3.2	3.5	4.0	0.031	0.011	0.273	0.120
Geunhwa H.S.	1.5	1053	286	S_B	47.7	54.9	54.9	0.002	0.001	0.143	0.051
Hwangsung E.S.	12	521	337	S_C	7.0	4.9	6.5	0.112	0.018	0.197	0.073
Kyeongju H.S.	16	563	436	S_C	6.8	8.0	8.5	0.008	0.002	0.213	0.077
Kyeonghee S.	20	506	420	S_C	5.3	6.4	6.9	0.035	0.011	0.262	0.094
Industrial S.	36	439	468	S_C	3.3	4.0	4.5	0.116	0.020	0.260	0.097
Shinla H.S.	7	1239	617	S_B	22.0	22.3	22.8	0.004	0.001	0.173	0.062
Youth Center	16	487	354	S_C	5.5	5.9	6.8	0.020	0.005	0.241	0.094
Wallsung E.S.	40	411	447	S_C	2.8	2.9	3.4	0.029	0.007	0.187	0.073
Banwall Palace	14	466	264	S_C	4.7	4.4	5.6	0.281	0.048	0.262	0.104

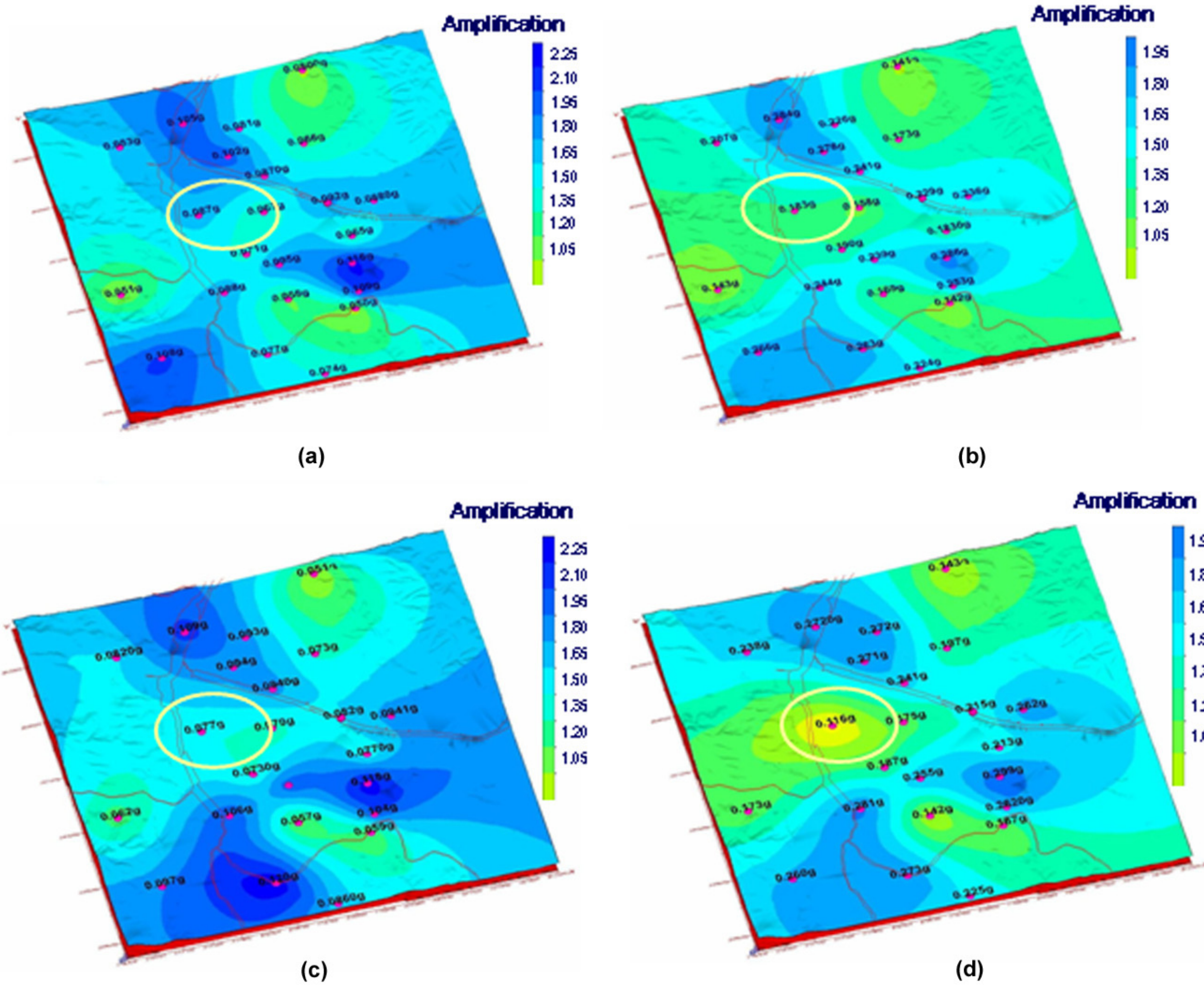

Fig. 10. Distribution map of site amplification for the peak acceleration from equivalent linear analysis (SHAKE) (a) Rock-outcrop motion of 0.05*g* (El Centro EQ, OLE), (b) Rock-outcrop motion of 0.14*g* (El Centro EQ, CLE), (c) Rock-outcrop motion of 0.05*g* (Artificial EQ, OLE), (d) Rock-outcrop motion of 0.14*g* (Artificial EQ, CLE).

layers which are common in central Kyeongju area show high potentials for amplification. Fig. 10 shows the distribution maps of site amplification for the peak acceleration constructed by GIS tools. The numbers written in the figure indicate the peak ground accelerations of the sites and the amplification ratio to the peak rock-outcrop acceleration can be identified with darkness of contour.

As expected, site amplification of basin area is much greater than that of mountain area in general. However, it is not shown that the low mean shear wave velocity sites always have the high potential of site amplification. The central part (Green Zone) of studied area marked in Fig. 10 can be classified as S_D site, where $\bar{V}_S$ is low as shown in Fig. 8, but the amount of amplification is less than expected. Site amplification is affected not only by the mean shear wave velocity (softness of site) but also by the various parameters such as the shape of shear wave velocity profile with depth, input earthquake, nonlinearity of soil and so on. For the comparison purpose, linear analysis was also performed for each site and the variations of accelerations and shearing strains with depth at Green Zone and Hwangsung Park sites were plotted in Figs. 11 and 12, respectively. In the case of equivalent linear analysis, the variations in normalized modulus (G/G_{max}) with depth were also included. At Green Zone, the shearing strain amplitude increases significantly up to 0.6% at a depth of 3–9 m which is the soft layer, and the normalized modulus (G/G_{max}) reduces to the value of 0.106. Consequently, the earthquake energy is substantially absorbed in the soft layer and the amplification of ground acceleration is much lower. This phenomenon is conspicuously shown on the CLE behaviors based on equivalent linear analysis (SHAKE) at Green Zone while the amplification is significant in the linear analysis because of no-reduction of shear modulus. In the case of Hwangsung Park where the stiffness of soil increases gradually with depth, the

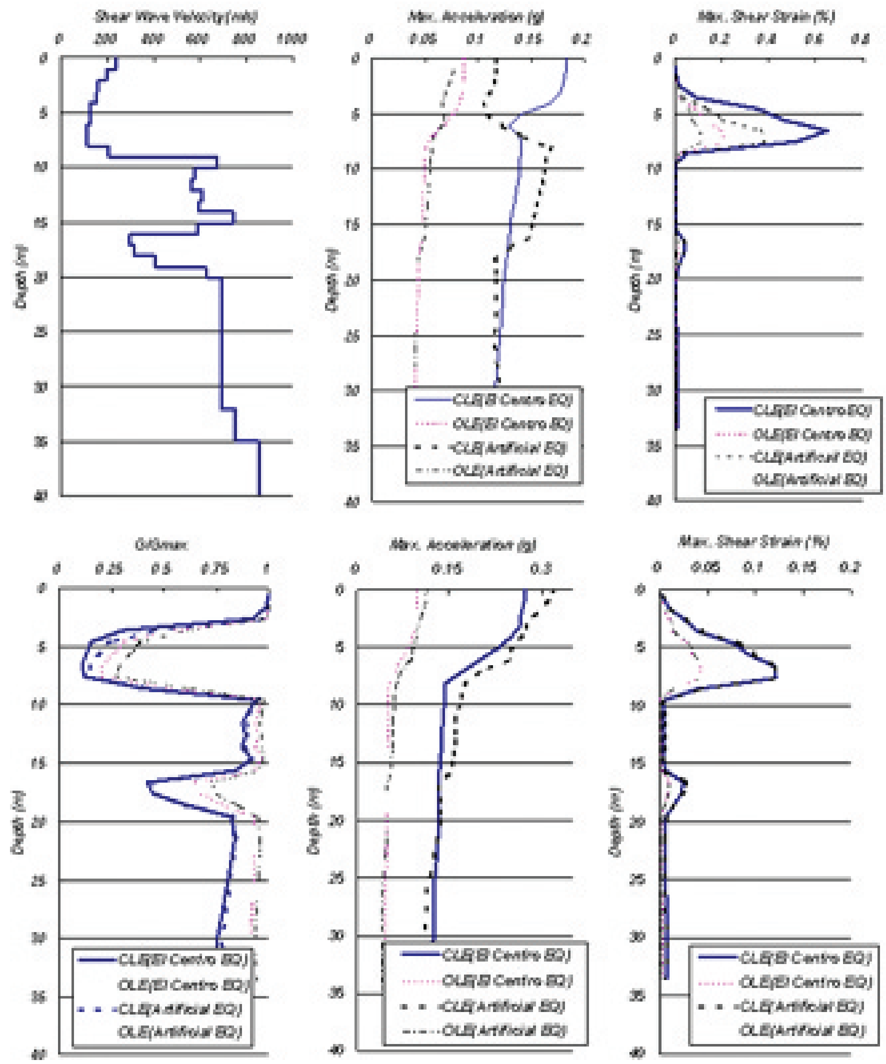

Fig. 11. The ground response analysis result of Green Zone (a) V_S profile, (b) Max. acceleration (SHAKE), (c) Max. shear strain (SHAKE), (d) G/G_{max} (SHAKE), (e) Max. acceleration (Linear), (f) Max. shear strain (Linear).

amplification of acceleration from bedrock to surface is considerably high even in the equivalent linear analysis on CLE (Fig. 12). In this case, the induced strain level is lower and the normalized modulus is higher compared with those in Green Zone.

Distribution maps of site amplifications and peak ground acceleration determined by linear analysis are shown in Fig. 13. The amplification ratios on CLE are identical with those on OLE because the nonlinearity of soil cannot be considered in the linear analysis. Compared with the amplification in Fig. 10, the ground surface accelerations determined by linear analysis were significantly larger than those determined by equivalent linear analysis, particularly on CLE. The importance of considering nonlinearity of soil can be assessed in these comparisons.

Comparisons between typical response spectra of rock-outcrop and ground surface motions to the standard response spectrum of S_C sites are shown in Fig. 14. The amplification is shown particularly near natural period of 0.1–0.2 s and the spectral acceleration of ground surface is higher than the standard spectrum. The amplification of ground motions of the level site is significantly affected by the natural period of the site depending upon the dynamic stiffness and the depth to bedrock, and approximately estimated by:

$$T_n = 4H/V_S^* \quad (1)$$

where, T_n is the natural period, H is the depth to the bedrock, and V_S^* is the average shear wave velocity to the bedrock. As given in Eq. (1), it must be preceded to examine the soil profile depth to the bedrock for the estimation of natural site period. The comparisons between natural periods

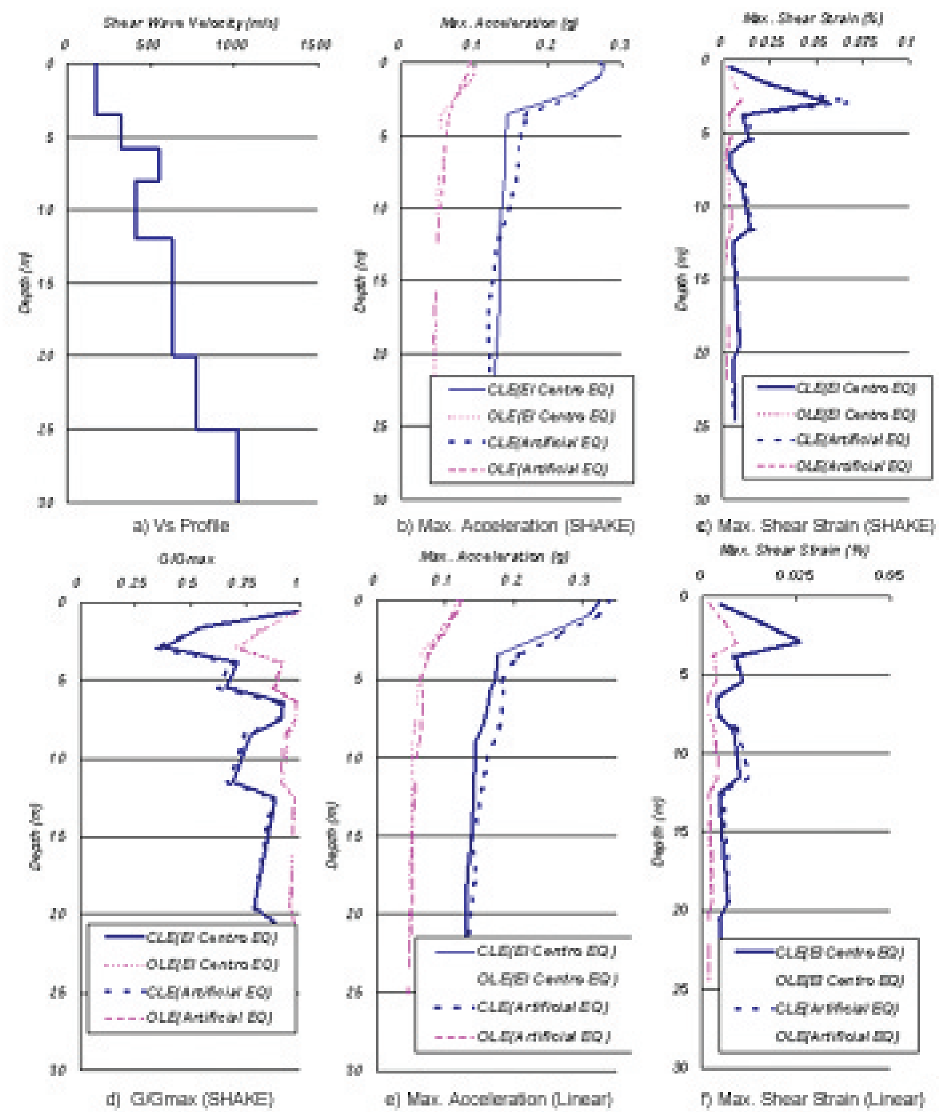

Fig. 12. The ground response analysis result of Hwangsung Park (a) V_S profile, (b) Max. acceleration (SHAKE), (c) Max. shear strain (SHAKE), (d) G/G_{max} (SHAKE), (e) Max. acceleration (Linear), (f) Max. shear strain (Linear).

determined by ground response analysis and by the estimation using Eq. (1) are shown in Fig. 15. Both natural periods match reasonably, and it can be mentioned that the resonance region of the site can be estimated by using the depth of site with the average shear wave velocity. Nevertheless, for the more exact determination of natural period of the specific site, the ground response analysis is carried out considering soil nonlinearity.

In this study, the dominant periods of the wide target area were estimated based on the interpolated bedrock profiles and average shear wave velocities in three dimension using GIS tool. In Fig. 16, the distribution map of the dominant site period is compared with the building distribution. Generally, natural period of building is 0.1 times its own story. Therefore, it can be mentioned that 2–5 story buildings in Kyeongju which have the similar natural period with the site may be susceptible for resonance during earthquakes, and it is recommended to consider the counter plan against the seismic hazard.

Among 28 sites at Kyeongju, 3, 21, and 4 sites are classified as S_B, S_C, and S_D, respectively, and the mean response spectra of S_B, S_C and S_D sites were compared to the spectra of S_B, S_C and S_D sites specified in the code (Fig. 17). In the case of S_C sites, spectral accelerations in period range of 0.04–0.30 s are significantly higher than in the standard design response spectrum. In the case of S_D sites, spectral accelerations in period range of 0.2–0.5 s are a little higher than in the standard design response spectrum. At a long period above about 0.8 s, both estimated spectral accelerations for S_C and S_D sites are much lower than those in the

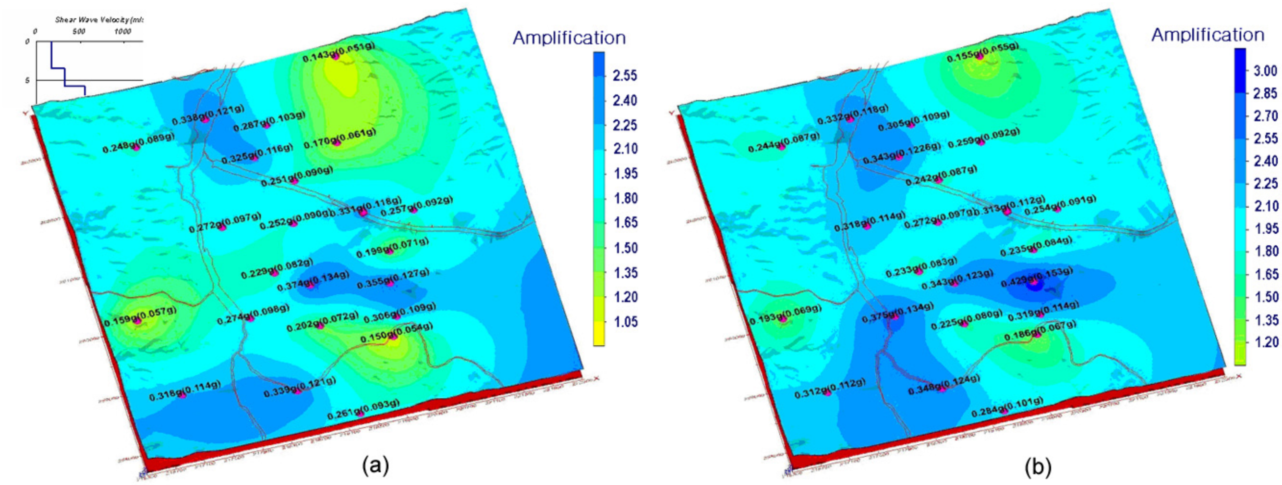

Fig. 13. Distribution maps of site amplifications and the peak ground accelerations from linear analysis (a) El Centro EQ on CLE (OLE), (b) Artificial EQ on CLE (OLE).

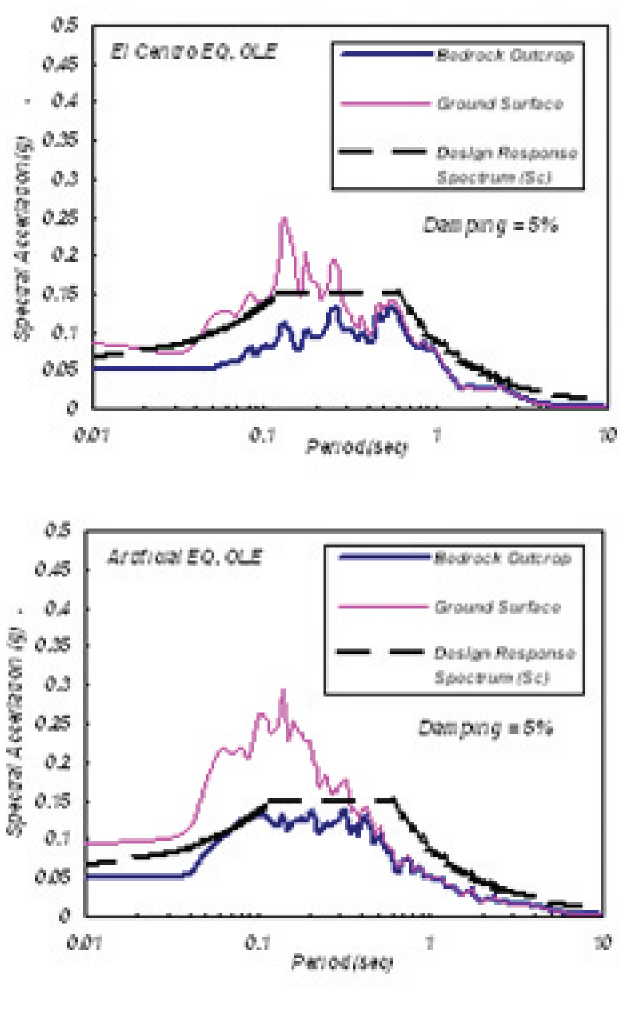

Fig. 14. Typical response spectra of rock-outcrop and ground surface motions (Youth Center).

standard design spectrum. Because site-specific evaluation of design response spectra requires various influencing factors that should be properly considered and only a few site-specific analyses were performed, these comparisons provide preliminary result, but it is interesting to investigate the site-specific degree of amplification at Kyeongju.

The evaluation of ground motion in Korean seismic design guide is quite similar to the method in Uniform building code (UBC) [7]. Borcherdt [3,4] has defined the short and mid-period amplification factors (F_a and F_v) as follows:

$$F_a(\mathrm{RRS}) = \frac{R_{soil}}{R_{rock}} \frac{1}{0.4} \int_{0.1}^{0.5} \frac{\mathrm{RS}_{soil}(T)}{\mathrm{RS}_{rock}(T)} \mathrm{d}T \tag{2}$$

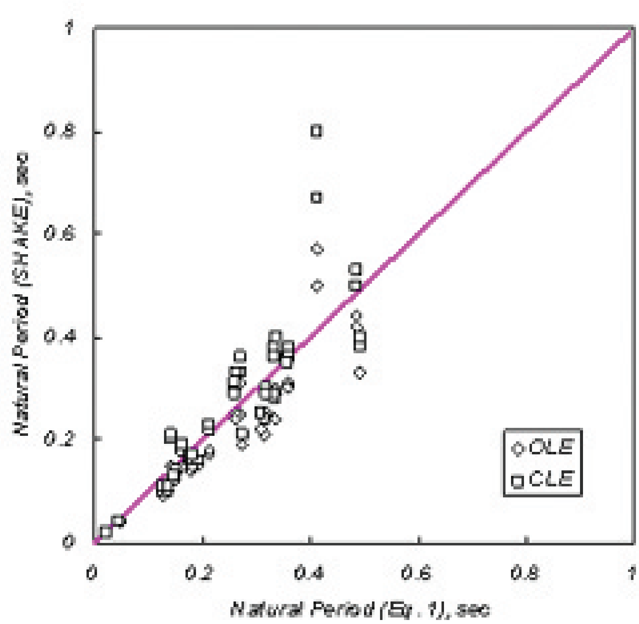

Fig. 15. Comparisons of natural periods determined by ground response analysis and by the estimation using Eq. (1).

$$F_v(\mathrm{RRS}) = \frac{R_{\mathrm{soil}}}{R_{\mathrm{rock}}}\frac{1}{1.6}\int_{0.4}^{2}\frac{\mathrm{RS}_{\mathrm{soil}}(T)}{\mathrm{RS}_{\mathrm{rock}}(T)}\,\mathrm{d}T \quad (3)$$

where $\mathrm{RS}_{\mathrm{soil}}$, $\mathrm{RS}_{\mathrm{rock}}$ are response spectra on soil and rock at a given period T, and R_{soil}, R_{rock} are distances of soil and rock station to the zone of largest energy release on the fault at a depth of about 18 km. The ratio of $R_{\mathrm{soil}}/R_{\mathrm{rock}}$ was assumed to be 1.0 in this paper.

The ratio of response spectra (RRS) of S_C and S_D sites and amplification factors, F_a and F_v based on UBC are shown in Fig. 18. In S_C sites, F_a value based on UBC is underestimated and F_v value based on UBC is overestimated compared with RRS value of S_C sites at Kyeongju. Especially, there is nearly no amplification in the range of period 1–2 s. In S_D sites, F_a value based on UBC is reasonable when compared with the case of S_C sites. But in long period range, F_v value based on UBC is too overestimated when compared with RRS of S_D sites at Kyeongju.

The distribution map of amplification factors, F_a and F_v, are shown in Figs. 19 and 20, respectively, and the amplification factors, F_a and F_v are plotted with the mean shear wave velocity of the upper 30 m in Fig. 21.

The calculated F_a values were larger, whereas the calculated F_v values were smaller than those in UBC in most cases. Generally in Korea, the depth to bedrock is shallow, the soil stiffness is medium to stiff and thereby the natural period of a site ranges between 0.1 and 0.5 s. Therefore, the mid-period amplification factor is small compared with UBC. On the contrary, the short period amplification factor is larger than UBC because the natural periods of S_C sites are in the range of 0.1–0.3 s. The site-specific amplification factors (F_a and F_v) of Kyeongju for input ground motion levels between $0.05g$ and $0.14g$ were estimated by the regression curves as shown in Fig. 21. At several sites, the mean shear wave velocities for the upper 30 m were close to 360 m/s as shown in Table 1 and the sites were classified as either S_C or S_D even though the difference in the mean shear wave velocity is small. Because the mean velocity for the upper 30 m ranges mostly between 300 and 600 m/s in Korea, it is recommended that the site classes be divided more closely or the site amplification factors for the construction of response spectrum be selected directly based on the mean shear wave velocity using the regression curves.

Since there are few earthquake data concerning soil effects, it is difficult to construct reliable seismic design guide in Korea. Based on this study, it is thought that the existing Korean seismic design guide based on UBC need to be modified for the reliable site amplification factors and the consideration of resonance frequency of a site. Site amplification is affected by various parameters, and the reliable site investigations

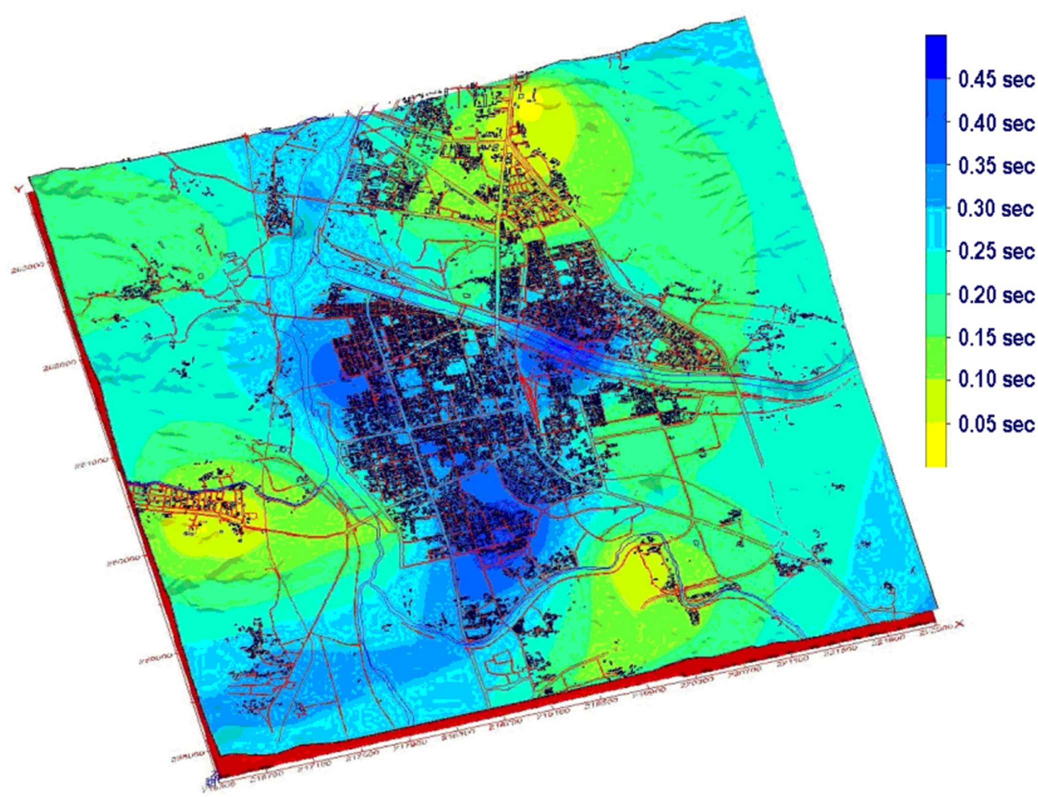

Fig. 16. Dominant site period map and buildings.

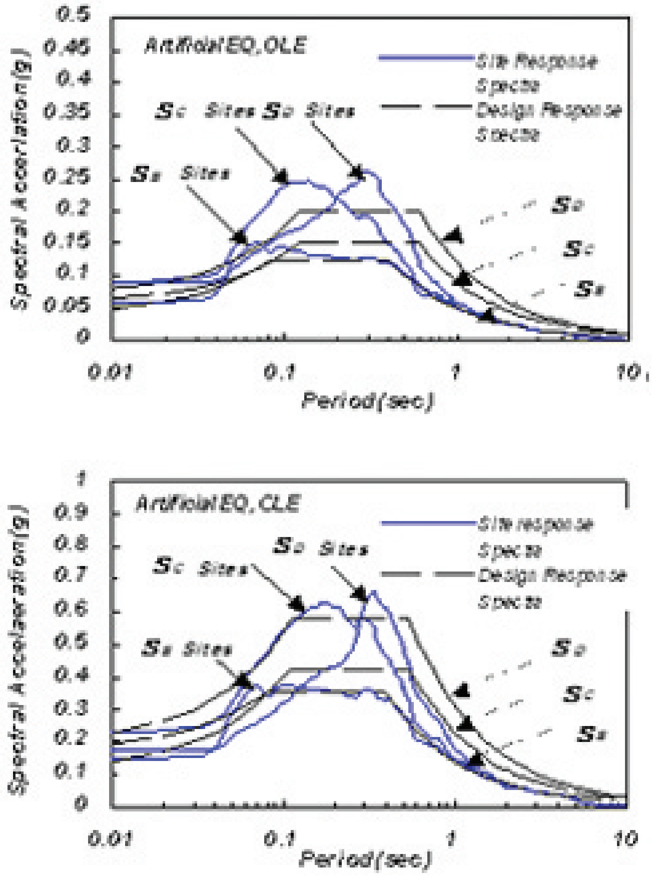

Fig. 17. Comparison of response spectra on sites and for design.

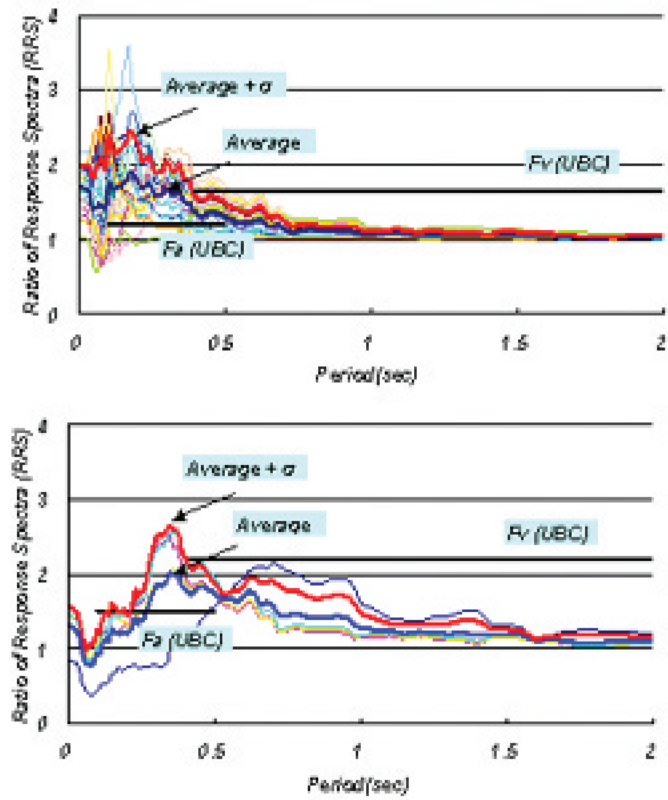

Fig. 18. RRS of S_C and S_D sites.

and characterization are essential. Especially, the evaluation of the reliable representative shear wave velocity profile of the site is crucial, because site amplification is much more affected by the shape of shear wave velocity profiles. Another important factor for reliable seismic guide is the frequency content of earthquake motions and it is required to construct input earthquake data that are suitable for the Korean peninsula. Further studies on the reliable site characterization, ground response analysis, and GIS application are underway.

6. Conclusions

Site characterization was performed at 10 km × 10 km

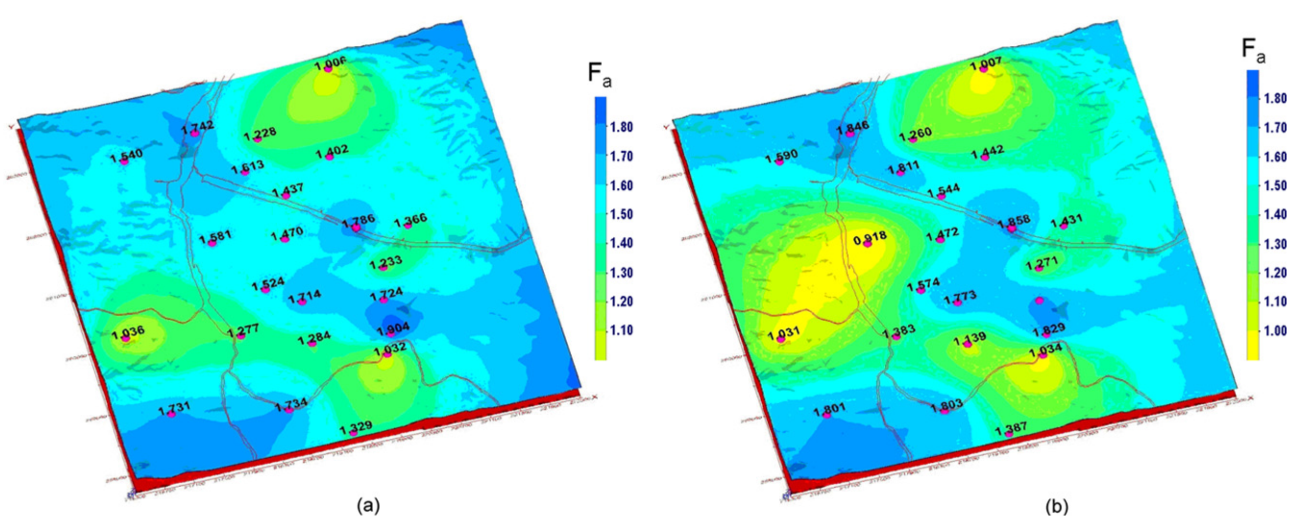

Fig. 19. Distribution map of short period amplification factor (F_a) (a) Artificial OLE earthquake, (b) Artificial CLE earthquake.

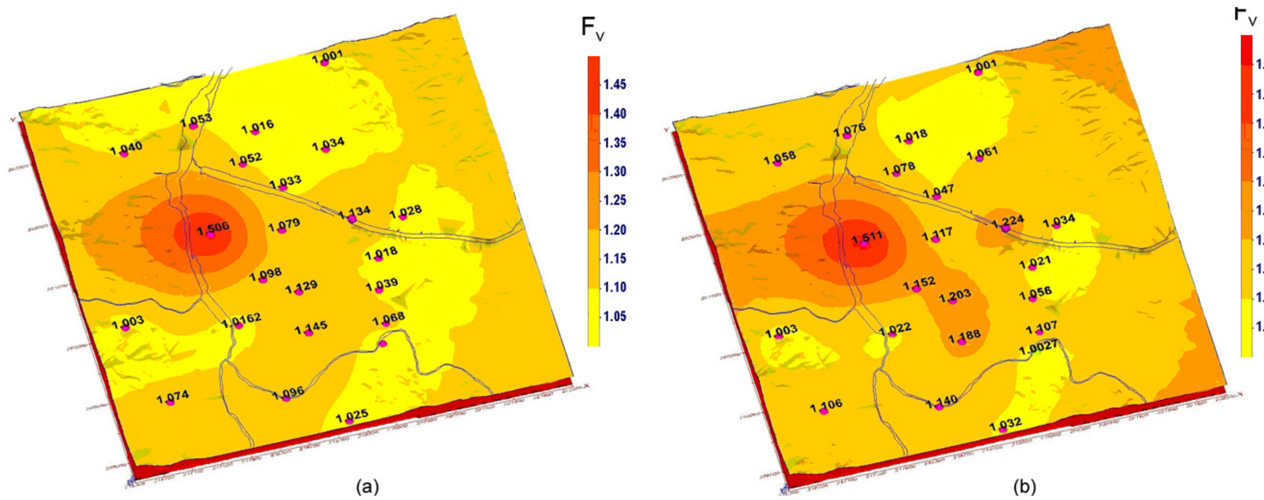

Fig. 20. Distribution map of mid-period amplification factor (F_v) (a) Artificial OLE earthquake, (b) Artificial CLE earthquake.

area around Kyeongju by using in situ and laboratory tests for the evaluation of earthquake ground motion. Kyeongju is located on a deep alluvial deposit composed by various floodings, and most sites are categorized as S_C and S_D based on Korean seismic design guide. Based on the equivalent linear analysis, the peak ground accelerations range between 0.141*g* and 0.299*g* on CLE and between 0.050*g* and 0.120*g* on OLE, respectively, showing high potential of amplification in the deep alluvial layer which is common in Kyeongju basin. Distribution maps of site amplification for the peak acceleration, amplification factors (F_a and F_v) and dominant site period of Kyeongju were constructed using GIS tools. The amplification factor based on the Korean seismic design guide underestimated the motion in short-period range and overestimated the motion in mid-period range in Kyeongju. The existing Korean seismic guide is required to be modified for the reliable site amplification factors and the consideration of resonance frequency of a site.

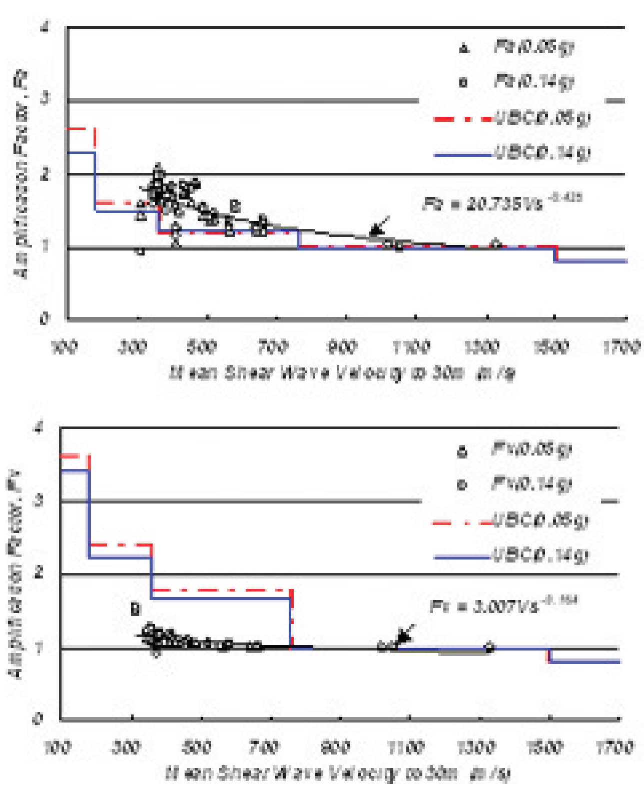

Fig. 21. Amplification factors (F_a and F_v) based on RRS of Kyeongju.

Acknowledgements

This study partially supported by Korea Institute of Nuclear Safety, Korea Electric Power Research Institute and Korea Earthquake Engineering Research Center are gratefully acknowledged.

References

[1] Adams T. Issues in GIS-based subsurface data management. Geographic information systems and their applications in geotechnical earthquake engineering. Atlanta, Georgia: ASCE, 1993 p. 12–6.
[2] ANSS Technical Integration Committee. Technical guideline for the implementation of an advanced national seismic system, 2001 (http://www.anss.org).
[3] Borcherdt RD. Preliminary amplification estimates inferred from strong ground-motion recordings of the Northridge earthquake of January 17, 1994. Proceedings of the International Workshop on Site Response Subjected to Strong Earthquake Motion, vol. 2; 1996. p. 21–46.
[4] Borcherdt RD. Estimates of site-dependent response spectra for new and existing highway facilities (methodology and justification). Proceedings of the NCEER Workshop on the National Representation of Seismic Ground Motion for New and Existing Highway Facilities, San Francisco; 1997.
[5] Dobry R, Ramos R, Power MS. Site factors and site categories in seismic codes. Technical Report MCEER-99-0010, MCEER; 1999.
[6] Idriss IM, Sun JI. User's manual for SHAKE91. Department of Civil

and Environmental Engineering, University of California, Davis; 1992.
[7] International Conference of Building Officials. 1997 Uniform building code, vol. 2 (structural engineering design provision); 1997.
[8] Kiremidjian AS. Spatial analysis in geotechnical earthquake engineering. Spatial analysis in soil dynamics and earthquake engineering, ASCE geotechnical special publication no 67 1997 p. 1–14.
[9] Lee KR. Historical records of three kingdoms by Kim Boo-Sik, Hangil, 1998 (in Korean).
[10] Lumb P. The properties of decomposed granite. Geotechnique 1962; 12(3):226–43.
[11] Martin GM, editor. Proceedings of the NCEER/SEAOC/BSSC Workshop on Site Response during Earthquakes and Seismic Code Provisions. University of Southern California, LA; 1994.
[12] Ministry of Construction and Transportation, Korea. Study of seismic design guidelines; 1997 (in Korean).
[13] Oliver MA, Webster R. Kriging: a method of interpolation for geographical information systems. Int J Geogr Inf Syst 1990;4(3): 313–32.